General Disclaimer

One or more of the Following Statements may affect this Document

- This document has been reproduced from the best copy furnished by the organizational source. It is being released in the interest of making available as much information as possible.

- This document may contain data, which exceeds the sheet parameters. It was furnished in this condition by the organizational source and is the best copy available.

- This document may contain tone-on-tone or color graphs, charts and/or pictures, which have been reproduced in black and white.

- This document is paginated as submitted by the original source.

- Portions of this document are not fully legible due to the historical nature of some of the material. However, it is the best reproduction available from the original submission.

NASA

Technical Memorandum 85036

ORDINARY MODE AURORAL KILOMETRIC RADIATION-WITH HARMONICS-OBSERVED BY ISIS 1

Robert F. Benson

MAY 1983

National Aeronautics and
Space Administration

Goddard Space Flight Center
Greenbelt, Maryland 20771

ORDINARY MODE AURORAL KILOMETRIC RADIATION - WITH HARMONICS - OBSERVED BY ISIS 1

Robert F. Benson

Laboratory for Planetary Atmospheres

NASA/Goddard Space Flight Center

Greenbelt, MD 20771

May 1983

Presented at the National Radio Science Meeting in Boulder, Colorado (January 1983).

Accepted for publication in Radio Science (special issue) on emissions from particle beams in space).

Abstract

ISIS 1 topside-sounder receiver observations that reveal examples of o-mode auroral kilometric radiation (AKR) are presented. They correspond to locations outside of the low density source region of intense AKR x-mode emission. The propagation modes are identified by comparing the natural radiation wave cutoffs with the local resonant and wave cutoff phenomena stimulated by the sounder transmitter. The o-mode AKR is the dominant emission in these regions of relatively high electron density, but it is considerably weaker than the intense x-mode AKR observed to emanate from low density cavities above the auroral regions. In addition to the fundamental o-mode, 2nd and 3rd harmonic bands of radiation have also been detected. Harmonics associated with these o-mode AKR are less intense than the harmonics associated with x-mode AKR. It is difficult to explain the variety of harmonic AKR observations (x as well as o-mode) based on present AKR theories.

CONTENTS

INTRODUCTION

Many theories have been proposed to explain auroral kilometric radiation (AKR) - the most intense emission of natural origin from the terrestrial magnetosphere (see the review by Grabbe [1981]). The main theoretical challenge has been to explain this great emission intensity which indicates that a particle to wave energy conversion process with an efficiency as large as 1% is involved [Gurnett, 1974; Benson and Calvert, 1979; Green et al., 1979]. The propagation mode and harmonic components of the radiation are among the most important theoretical parameters amenable to observational confirmation. One theoretical approach, based on direct amplified cyclotron emission [Melrose, 1976; Wu and Lee, 1979], predicts radiation in both extraordinary and ordinary modes, both with harmonics, with the fundamental x-mode being by far the dominant signal in the low density source regions of intense AKR (Melrose et al., 1982]. Most observations have inferred that the main radiation is in the x-mode [Gurnett and Green, 1978; Kaiser et al., 1978; Benson and Calvert, 1979; Shawhan and Gurnett, 1982]. The plasma wave receiver on the Jikiken satellite (EXOS-B) also detects AKR [Morioka et al., 1981]. In this case, however, the dominant radiation is interpreted to be in the o-mode (Oya and Morioka, private communication, 1983).

The reason for this apparent discrepancy in AKR polarization determinations may be due to the different vantage points of the observing platforms relative to the source region of intense AKR. A number of investigations have placed the location of this source region along auroral field lines at geocentric distances between about 1.5 and 3.5 R_e [Gurnett, 1974; Kurth et al., 1975; Green et al., 1977; Alexander et al., 1979; Benson and Calvert, 1979; Gallagher and Gurnett, 1979; Morioka et al., 1981; Calvert, 1981b]. All of the AKR observations interpreted as x-mode were either made from polar

orbiting satellites or from spacecraft very distant from the earth so that radiation from the polar regions could be directly received. The Jikiken satellite, on the other hand, had an inclination of only 31^{o} and an apogee of about 5 R_e. Thus the observations in this case are largely confined to the equatorial side of the source region for intense AKR.

The purpose of the present paper is to show examples of AKR as observed by ISIS 1 when it is near - but outside of - the source region for intense x-mode AKR. Under these conditions, it is found that the o-mode AKR is often dominant. In addition, harmonic AKR bands are observed to be associated with this o-mode radiation as have been observed with (presumably) x-mode AKR from ISIS 1 [Benson and Calvert, 1979; Benson, 1982] and ISEE (R. Anderson, private communication, 1982).

OBSERVATIONS

The signature of AKR on ISIS 1 ionograms has been described by Benson and Calvert [1979], Benson [1981], Calvert [1981a] and (in a comparison paper in this issue) Benson and Akasofu [1983]. ISIS 1 does not have the capability to make polarization measurements. Polarization information can be inferred, however, by comparing the observed wave cutoffs of radiation received from natural sources (such as AKR) with the local resonant and wave cutoff phenomena stimulated by the sounder transmitter. This process is schematically illustrated in Figure 1.

The left side of Figure 1 corresponds to an encounter with the source region of intense x-mode AKR. In this case the electron density N_e is so low that the plasma frequency f_N is below the low frequency instrumental cutoff of 0.1 MHz, i.e., $N_e < 100$ cm^{-3} since f_N (kHz) $\simeq 9$ $[N_e\ (cm^{-3})]^{1/2}$. Under these conditions the sounder-stimulated electrostatic resonance at the upper hybrid

frequency f_T and the cutoff frequency f_x for the electromagnetic x-mode coalesce with the stimulated resonance at the local electron gyrofrequency f_H since $f_T^2 = f_H^2 + f_N^2$ and $f_x = (f_H/2)\ (1 + [1 + 4\ f_N^2/f_H^2]^{1/2}) \simeq f_H\ (1 + f_N^2/f_H^2)$ when $4\ f_N^2/f_H^2 << 1$. In addition, harmonic AKR bands are observed very close to the stimulated nf_H resonances. See the discussion in connection with Figure 1 of the companion paper [Benson and Akasofu,1983] for further details.

The right side of Figure 1 corresponds to a situation where the ambient value for N_e is considerably greater so that the f_N resonance is now visible on the ionogram above the 0.1 MHz lower frequency limit (although it is still less than f_H). The frequencies f_H, f_T and f_x are now clearly separated as are the harmonic resonances at $2f_H$ and $2f_T$. The nonlinear processes responsible for these harmonic resonances are attributed to phenomena taking place in the ambient medium rather than the instrumentation [Benson, 1982b].

The processes responsible for the harmonic AKR noise bands associated with the fundamental x-mode AKR noise band (Figure 1, left) are also attributed to phenomena taking place in the ambient medium rather than the instrumentation [Benson, 1982a]. The observations to be presented here will provide evidence that similar comments hold in regard to the harmonics associated with the fundamental o-mode AKR noise band (Figure 1, right). These harmonics will be referred to as o-mode harmonics even though they are observed above f_x and thus could be either x or o-mode. A justification for this terminology will be given based on the frequency structure in these harmonic bands which is observed to correspond to harmonics of the frequency structure of the fundamental o-mode AKR band.

An example of o-mode AKR, as detected by ISIS-1, has been presented earlier (see Figure 10 of Benson [1982a]). In this example, f_N/f_H was only 0.3. The separation between f_H and f_x (schematically illustrated on the right

side of Figure 1) under these conditions is at the threshold of resolution. Nevertheless, the fundamental AKR band could be identified as o-mode because it was observed in the frequency range below f_H (and hence below f_x). Second and third harmonic noise bands were also observed; they were observed just below the ambient values for $2f_H$ and $3f_H$, respectively. These observations were interpreted in terms of a source region extending from the satellite altitude to higher altitudes where f_H was less than the ambient value at the satellite. This interpretation is consistent with the conclusions reached in the companion paper which presents N_e altitude contours through the AKR source region for this event (see the discussion related to Figure 6 of Benson and Akasofu [1983]). Another example of o-mode AKR when $f_N/f_H = 0.3$ was presented in this companion paper (see Figure 7a of Benson and Akasofu [1983]). In this case, however, there could be a mixture of o and x-mode AKR because the fundamental noise band extended to frequencies well above f_x (which is merged into the high frequency side of f_H on the ionogram) as well as extending slightly below f_H. Similiarly, the 2nd and 3rd harmonic noise bands extend on both sides of the stimulated resonances at $2f_H$ and $3f_H$. The low frequency cutoff of the o-mode AKR near f_H, rather than near the o-mode propagation cutoff at f_N, is consistent with the theoretical results of Hewitt and Melrose [1983] that radiation near f_H is by far the most important and the results of Wu and Lee [1979] and Hewitt et al. [1982] that it is mainly directed upward.

Figures 2 and 3 present o-mode AKR examples recorded when $f_N/f_H = 0.4$ and 0.5, respectively. In each case, the fundamental AKR signal is clearly observed to exist only in the frequency region below the x-mode cutoff f_x. Second and third harmonic AKR bands are observed in Figure 3 as well as a signal below f_N which could be either in the whistler or the z-mode (the low frequency branch of the x-mode see, e.g., Budden, 1961). The 2nd harmonic AKR

signal in this example was strong enough to cause an automatic gain control (AGC) voltage change that desensitized the receiver to the point that the ionospheric echo was interrupted.

Figure 4 presents 3 ISIS 1 ionograms which were recorded under conditions of much higher electron density such that $f_N/f_H = 1.0$. They were taken from one of the passes examined in detail for AKR/aurora correlations in the companion paper of Benson and Akasofu [1983]. They correspond to satellite positions on the equatorward side of the steep latitudinal N_e gradients near 56° latitude in Figure 6 of that paper. The most striking features on the data presented in Figure 4, especially on the bottom 2 ionograms, are the frequency components on the fundamental o-mode AKR which are reproduced in the harmonic noise bands. The high frequency component dominates the low frequency component of the 2nd harmonic band, and a trace of a 3rd harmonic band appears at a location near that expected for the high frequency component. The 3rd harmonic signals are evident as slight enhancements of the AGC traces on the bottom 2 ionograms. These 2nd and 3rd harmonic AKR bands could be either o or x-mode because they are observed in the frequency range above f_x; they could even result from the reception of es emissions. In addition, the frequency structure observed in the fundamental and harmonic bands may result from the superposition of signals from more than one source involving more than one generation mechanism. If the observed signals result from a single mechanism, however, then the duplication of the frequency component structure of the fundamental in the harmonic bands suggests that they are related to the fundamental - which is here designated as the fundamental o-mode AKR band.

These harmonics associated with o-mode AKR have been observed up to the 3rd, e.g., see Figure 3. Those observed to be associated with what is

attributed to x-mode AKR, on the other hand, have been observed up to the 4th [Benson, 1982a]. A comparison between o and x-mode harmonics reveals that the x-mode is more intense. Even the fundamental o-mode is observed to be much less intense than the fundamental x-mode. The o-mode AKR is seldom strong enough to saturate the receiver AGC whereas it is typically saturated in the case of x-mode AKR. Based on earlier inspections of sounder receiver video amplitude records for cases of saturated AGC x-mode AKR [H. G. James, private communication, 1978; Benson and Calvert, 1979], the difference in received power between maximum intensity x-mode and maximum intensity o-mode AKR is about 30 dB. On those rare occasions when the o-mode AKR saturates the AGC voltage [Benson, 1983] the power difference could be considerably less. These relative strengths, between the o and x-mode fundamental and harmonic AKR bands, are illustrated schematically in Figure 1 by the level of shading of the video signals and by the level of the AGC traces.

DISCUSSION

Several theoretical studies have considered the generation of o-mode AKR; they fall into the following 3 groups: (1) the mode conversion theories of Benson [1975] (an adaptation of the Jovian decametric radiation theory of Oya [1974] to the terrestrial radiation) and Jones [1977], (2) the beam-driven electromagnetic instability [Palmadesso et al., 1976] and (3) the cyclotron instability [Melrose, 1976; Wu and Lee, 1979]. The first two have been largely discounted; the first because of the expected low overall energy conversion efficiency and the second because o rather than x-mode AKR was predicted (see the review by Grabbe [1981]). The third mechanism predicts o as well as x-mode but the former was discounted on the basis of a relatively low instability growth rate. Since the present discussion is concerned with

o-mode AKR, which is observed to be considerably less intense than x-mode AKR, all of the above theories should be re-examined based on the present observations.

None of the above theories, however, can explain the observed harmonic AKR components. Two mechanisms have been proposed which predict AKR specifically at $2f_H$: one is based on cyclotron solitons [Istomin et al., 1978; Cole and Pokhotelov, 1980] and the other on a coherent nonlinear 3-wave process [Roux and Pellat, 1979]. The cyclotron instability mechanism, on the other hand, can generate AKR at the fundamental and at the harmonics and the subject of harmonic AKR has been discussed by Lee et al. [1980], Melrose et al. [1982], Hewitt et al. [1982] and Hewitt and Melrose [1983]. The result of these investigations of the cyclotron instability mechanism is that the harmonics can become important at high plasma densities. For example, the x-mode 2nd harmonic dominates over the x-mode fundamental when $f_N/f_H \gtrsim 0.3$ and the o-mode 2nd harmonic dominates over the o-mode fundamental when $f_N/f_H \gtrsim 1.1$; in each case, however, the maximum instability temporal growth rates for the harmonics are about 2 orders of magnitude less than the values for the fundamentals (R. Hewitt, private communication, 1983). Even greater plasma densities are required for the higher harmonics to become important and they have, correspondingly, even lower growth rates.

Thus the cyclotron mechanism may explain the cases of 2nd harmonic AKR stronger than the fundamental or 2nd harmonic with no fundamental reported by Benson [1982a]. In these cases, propagation effects often seem to be important since they are observed over a wide latitude range [e.g., see Figure 2 of Benson and Akasofu, 1983]. It is difficult to explain multiple harmonics in the low density AKR source region with this mechanism, however, since the higher harmonics are only predicted to be significant in high density

regions. In this case propagation conditions do not appear to be important since multiple harmonics are only observed in the source region. This observation, which was first made by Benson and Calvert [1979], is vividly illustrated by the ionogram sequence in Figure 2 of the companion paper by Benson and Akasofu [1983]. Thus another mechanism may be operating in addition to the one generating fundamental AKR. Since propagation effects do not appear to be important in the case of the higher harmonics ($n > 2$), they may be electrostatic emissions resulting from beam-plasma interactions within the AKR source region as has been suggested by H. Oya (private communication, 1982).

If the emissions observed in Figure 4 are assumed to result from a single mechanism then the duplicate frequency structure observed in the fundamental, 2nd harmonic and (to a limited degree) the 3rd harmonic AKR bands suggests that the harmonics are caused by nonlinear processes acting on a single generated signal, namely the fundamental. This harmonic generation concept has been stressed by Calvert [1983]. In this regard, it is important to note that extreme density gradients are often observed in connection with such harmonics, e.g., see the N_e contours of Fig. 6 in the companion paper [Benson and Akasofu, 1983] which are relevant to Figure 4 of the present paper. Significant small scale density gradients may be present even when the sounder-derived N_e contours are smooth since such N_e structures cannot be resolved by the topside sounder. This point was illustrated in Figure 3 of Benson and Calvert [1979] where a comparison between N_e sounder and electrostatic probe measurements was made during an AKR source region encounter.

The present ISIS 1 observation of o-mode fundamental AKR are consistent with the o-mode AKR observed by Jikiken (Oya and Morioka, private communication, 1983) and the recent DE 1 results of Shawhan et al. [1983]. In each

case the observations are consistent with the ISIS 1 findings that the o-mode AKR originates from relatively high density regions, i.e., the former corresponds to observations equatorward of the main AKR density cavity and the latter only detects upcoming o-mode AKR - consistent with a source in the higher density region well below the DE 1 altitude.

Acknowledgements. I am grateful to S. A. Curtis and R. G. Hewitt for helpful discussions. Photographic reproductions of the ISIS 1 ionograms were made by the National Space Science Data Center at the Goddard Space Flight Center.

REFERENCES

Alexander, J. K., M. L. Kaiser, and P. Rodriguez, Scattering of terrestrial kilometric radiation at very high altitudes, J. Geophys. Res., 84, 2619-2629, 1979.

Benson, R. F., Source mechanism for terrestrial kilometric radiation, Geophys. Res. Lett., 2, 52-55, 1975.

Benson, R. F., Auroral kilometric radiation source region observations from ISIS 1, in Physics of Auroral Arc Formation, Geophysical Monograph 25, pp. 369-379, American Geophysical Union, Washington, D.C., 1981.

Benson, R. F., Harmonic auroral kilometric radiation of natural origin, Geophys. Res. Lett., 9, 1120-1123, 1982a.

Benson, R. F., Stimulated plasma instability and nonlinear phenomena in the ionosphere, Radio Sci., 17, 1637-1659, 1982b.

Benson, R. F., Characteristics of auroral kilometric radiation as a function of source region plasma parameters, EOS, 64, 270, 1983.

Benson, R. F., and S.-I. Akasofu, Auroral kilometric radiation/aurora correlation, Radio Sci., in press, 1983, also NASA Technical Memorandum 85035, Goddard Space Flight Center, Greenbelt, MD 20771, May, 1983.

Benson, R. F., and W. Calvert, ISIS 1 observations at the source of auroral kilometric radiation, Geophys. Res. Lett., 6, 479-482, 1979.

Budden, K. G., Radio Waves in the Ionosphere, 542 pp., Cambridge University Press, London, 1961.

Calvert, W., The signature of auroral kilometric radiation on ISIS 1 ionograms, J. Geophys. Res., 86, 76-82, 1981a.

Calvert, W., The auroral plasma cavity, Geophys. Res. Lett., 8, 919-921, 1981b.

Calvert, W., Current questions about auroral kilometric radiation, paper presented at the URSI National Radio Science Meeting, Boulder, Colorado, January, 1983.

Cole, K. D. and O. A. Pokhotelov, Cyclotron solitons-source of earth's kilometric radiation, Plasma Physics, 22, 595-608, 1980.

Gallagher, D. L., and D. A. Gurnett, Auroral kilometric radiation: time-averaged source location, J. Geophys. Res., 84, 6501-6509, 1979.

Grabbe, C. L., Auroral kilometric radiation: a theoretical review, Rev. Geophys. Space Res., 19, 627-633, 1981.

Green, J. L., D. A. Gurnett, and R. A. Hoffman, A correlation between auroral kilometric radiation and inverted V electron precipitation, J. Geophys. Res., 84, 5216-5222, 1979.

Green, J. L., D. A. Gurnett, and S. D. Shawhan, The angular distribution of auroral kilometric radiation, J. Geophys. Res., 82, 1825-1838, 1977.

Gurnett, D. A., The earth as a radio source: terrestrial kilometric radiation, J. Geophys. Res., 79, 4227-4238, 1974.

Gurnett, D. A. and J. L. Green, On the polarization and origin of auroral kilometric radiation, J. Geophys. Res., 83, 689-696, 1978.

Hewitt, R. G., and D. B. Melrose, Electron cyclotron maser emission near the cutoff frequencies, Aust. J. Phys., in press, 1983.

Hewitt, R. G., D. B. Melrose, and K. G. Ronnmark, The loss-cone driven electron-cyclotron maser, Aust. J. Phys., 35, 447-471, 1982.

Isotomin, Ya. N., V. I. Petviashvily, O. A. Pokhotelov, Terrestrial radio emission in the kilometer range by cyclotron solitons, Sov. J. Plasma Phys., 4, 76-78, 1978.

Jones, D., Mode-coupling of z-mode waves as a source of terrestrial kilometric and Jovian decametric radiations, Astron. Astrophys., 55, 245-252, 1977.

Kaiser, M. L., J. K. Alexander, A. C. Riddle, J. B. Pearce, and J. W. Warwick, Direct measurements by Voyagers 1 and 2 of the polarization of terrestrial kilometric radiation, Geophys. Res. Lett., 5, 857-860, 1978.

Kurth, W. S., M. M. Baumback, and D. A. Gurnett, Direction finding measurements of auroral kilometric radiation, J. Geophys. Res., 80, 2764-2770, 1975.

Lee, L. C., J. R. Kan, and C. S. Wu, Generation of auroral kilometric radiation and the structure of auroral acceleration region, Planet. Space Sci., 28, 703-711, 1980.

Melrose, D. B., An interpretation of Jupiter's decametric radiation and the terrestrial kilometric radiation as direct amplified gyroemission, Astrophys. J., 207, 651-662, 1976.

Melrose, D. B., K. G. Ronnmark, and R. G. Hewitt, Terrestrial kilometric radiation: the cyclotron theory, J. Geophys. Res., 87, 5140-5150, 1982.

Morioka, A., H. Oya, and S. Miyatake, Terrestrial kilometric radiation observed by satellite JIKIKEN (EXOS-B), J. Geomag. Geoelectr., 33, 37-62, 1981.

Oya, H., Origin of Jovian decameter wave emissions - conversion from the electron cyclotron plasma wave to the ordinary mode electromagnetic wave, Planet. Space Sci., 22, 687-708, 1974.

Palmadesso, P., T. P. Coffey, S. L. Ossakow, and K. Papadopoulos, Generation of terrestrial kilometric radiation by a beam-driven electromagnetic instability, J. Geophys. Res., 81, 1762-1770, 1976.

Roux, A. and R. Pellat, Coherent generation of the auroral kilometric radiation by nonlinear beatings between electrostatic waves, J. Geophys. Res., 84, 5189-5198, 1979.

Shawhan, S. D., and D. A. Gurnett, Polarization measurements of auroral kilometric radiation by Dynamics Explorer-1, Geophys. Res. Lett., 9, 913-916, 1982.

Shawhan, S. D., D. A. Gurnett, and R. L. Huff, Auroral zone wave emissions observed with Dynamics Explorer, paper presented at the URSI National Radio Science Meeting, Boulder, Colorado, January, 1983.

Wu, C. S. and L. C. Lee, A theory of the terrestrial kilometric radiation, Astrophys. J., 230, 621-626, 1979.

Figure Captions

Figure 1. Schematic illustrations of intense x-mode (left) and o-mode (right) AKR observed near source regions by ISIS 1. The electrostatic (es) ionospheric echoes (or sounder-stimulated plasma resonances) designated by N, H, nH, T and 2T correspond to f_N, f_H, nf_H, f_T and $2f_T$ respectively. The cutoff frequency f_x of the electromagnetic (em) x-mode ionospheric echo is designated by X. The plasma frequency f_N is the cutoff frequency for the em o-mode ionospheric echo. For clarity, this echo is not shown; it is normaly considerably weaker than the x-mode echo on topside-sounder ionograms. The flat top of the automatic gain control (AGC) voltage corresponds to the saturation level for this signal which is reached well before the ionogram video signal saturates.

Figure 2. Ordinary mode AKR observed by ISIS 1 on 8 December 1970 (the signal extending over all delay times in a narrow frequency band just below 0.5 MHz). The time corresponding to the f_H resonance was 2202:43 UT (0722 magnetic local time MLT, 3526 km altitude, 75.7° invariant latitude Λ, $f_N/f_H = 0.40$).

Figure 3. An ISIS 1 ionogram with o-mode AKR (the signal extending over all delay times just above 0.5 MHz) with 2nd and 3rd harmonics (the weaker signals just above $2f_H$ and $3f_H$, respectively). (August 7, 1969 0858:57 UT, 2212 MLT, 3137 km, 72.1° Λ, $f_N/f_H = 0.50$.)

Figure 4. Three ISIS 1 ionograms illustrating o-mode AKR with harmonics. The vertical arrows at the bottom straddling the 0.5 MHz frequency marker designate the locations of two distinct frequency components on the fundamental AKR band on the bottom two ionograms. These components are more apparent in the AGC trace because the 0.5 MHz frequency marker coincides with the minimum of the video signal. The sets of vertical arrows labeled 2 and 3 correspond to frequency multiples of the set of arrows labeled "1". Similarly, the horizontal arrows labeled 2 and 3 are multiples of the horizontal arrow labeled "1" which designates the frequency width of the fundamental AKR band. The ionograms were recorded on 31 October 1969 at 1356:43 UT (top - which corresponds to ionogram d of Figure 6 of Benson and Akasofu [1983]), 1358:07 UT (middle) and 1359:01 (bottom). The middle ionogram corresponds to 0159 MLT, 3221 km, 53.5° Λ and $f_N/f_H = 1.0$.

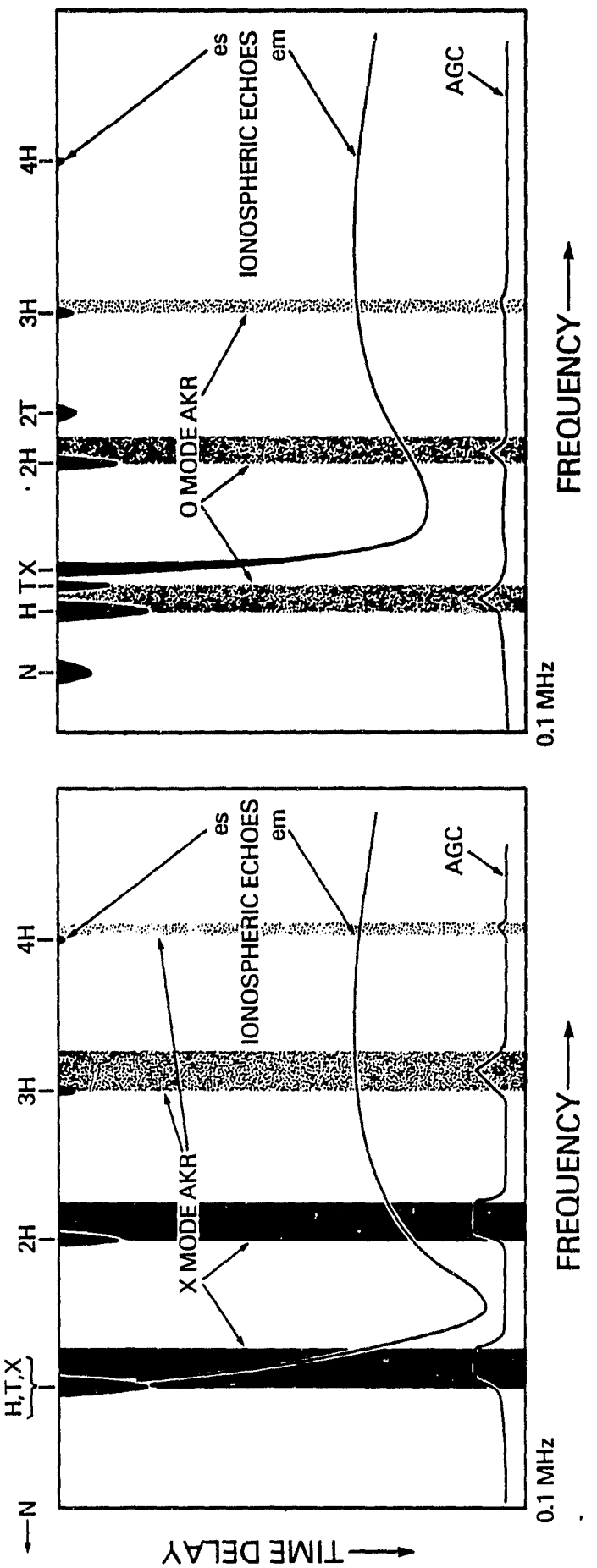

Figure 1

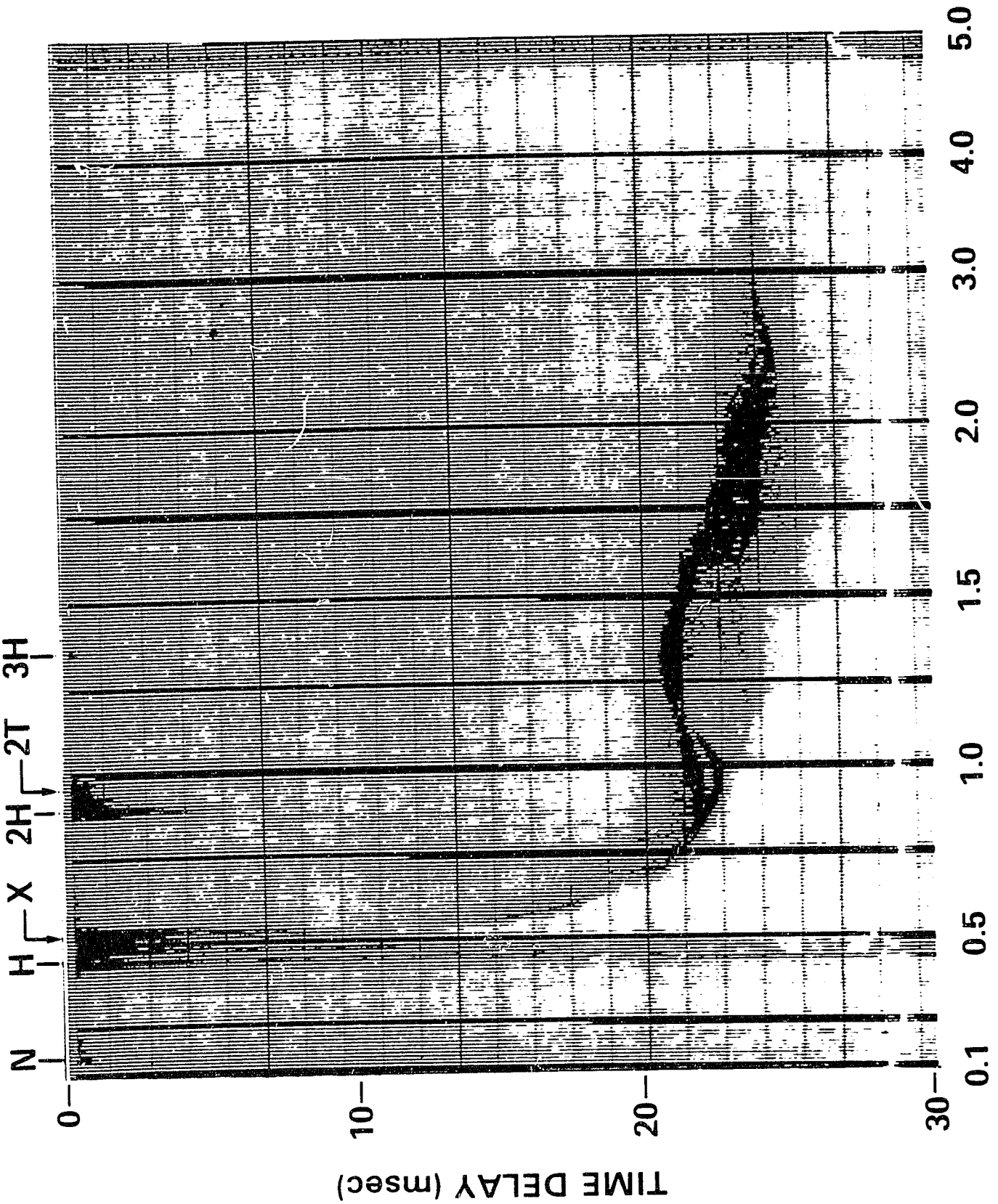

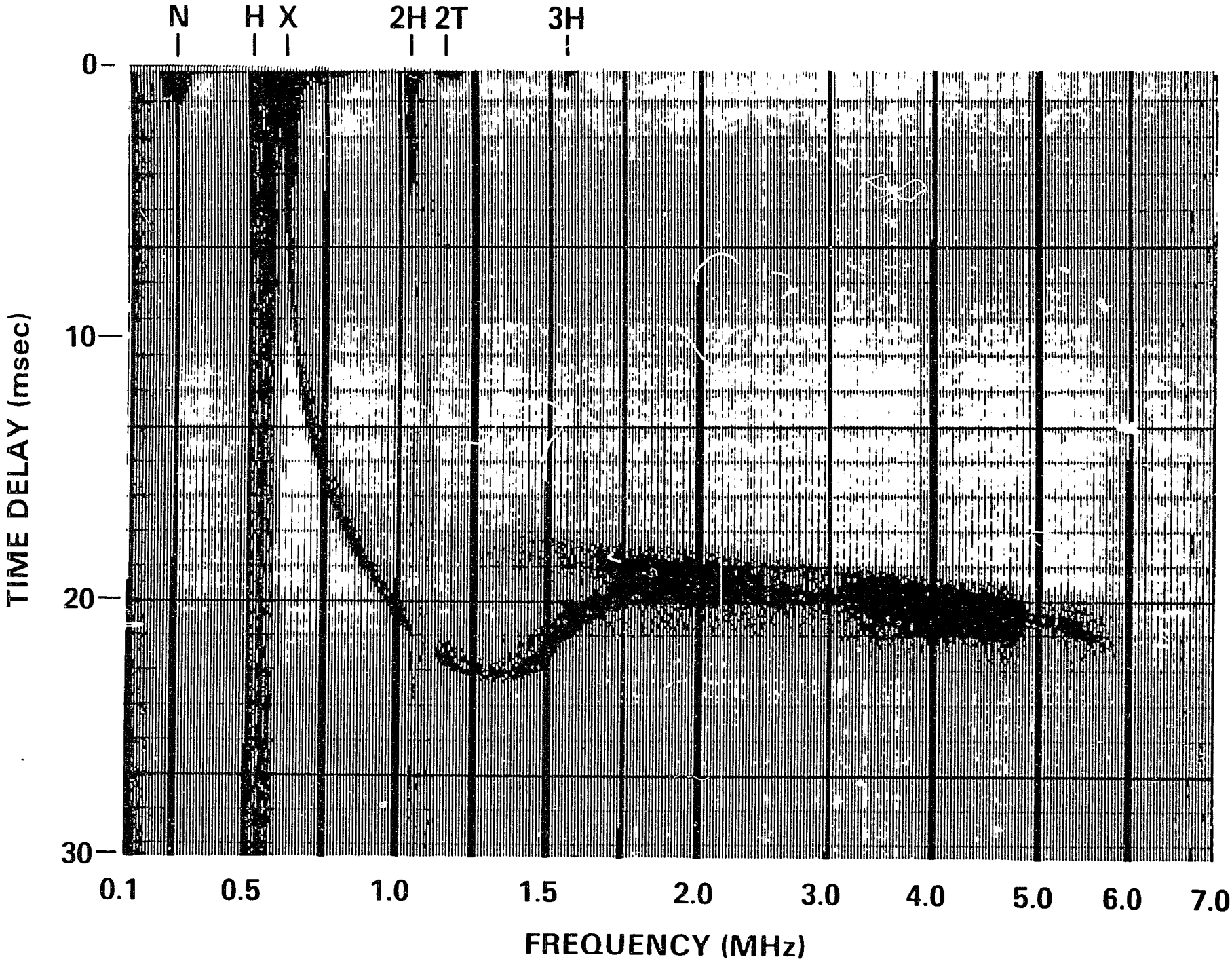

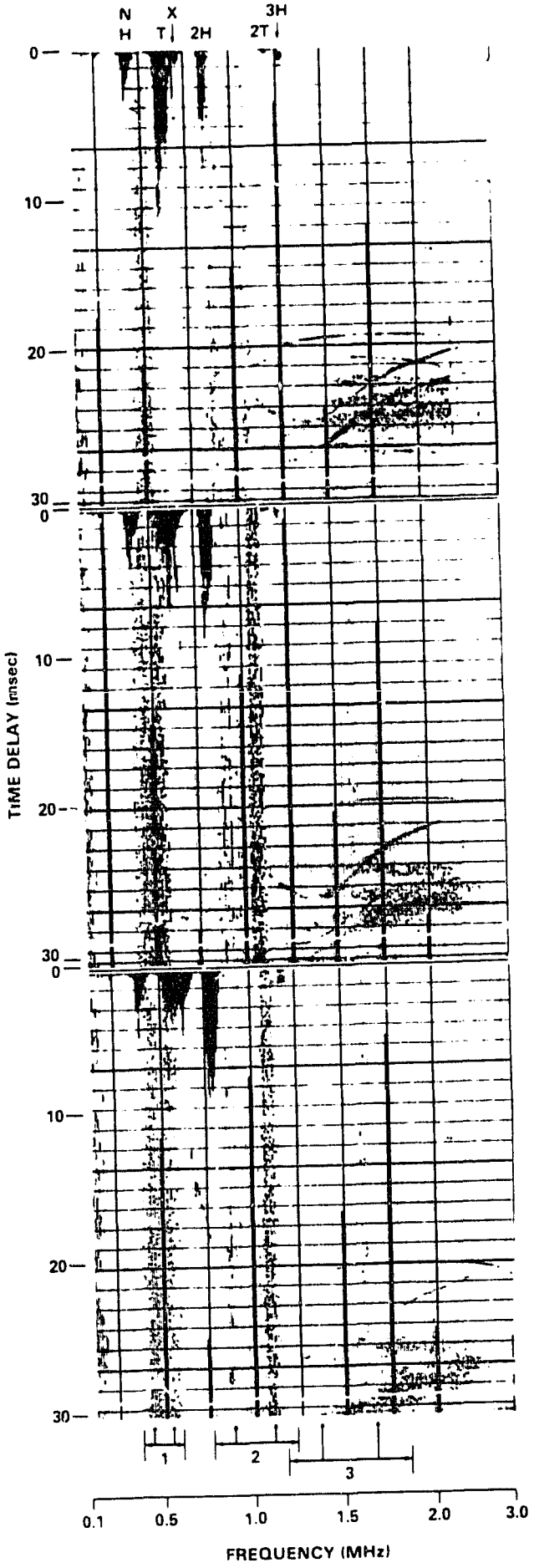

Figure 4